J Math Chem (2015) 53:604–617
DOI 10.1007/s10910-014-0440-z

ORIGINAL PAPER

Modelling dimer–dimer reactions on supported catalysts

V. Skakauskas · P. Katauskis

Received: 4 September 2014 / Accepted: 3 November 2014 / Published online: 12 November 2014

Abstract The kinetics of the dimer–dimer reaction, $2A_2 + B_2 \rightarrow 2A_2B$, proceeding on supported catalysts is studied numerically using a phenomenological model which includes: the bulk diffusion of reactants from a bounded vessel towards the adsorbent and the product bulk one from the catalyst surface into the same vessel, adsorption and desorption of particles of both reactants, and surface diffusion of adsorbed particles. Two different arrangements of adsorption sites were used: (i) the same total amount of active and inactive in the surface reaction adsorption sites, (ii) the same concentrations of active and inactive sites. Two adsorption cases of both reactants for each arrangement of adsorption sites are considered: (i) each reactant adsorbs on both active and inactive sites, (ii) both reactants adsorb only on the support. The model where concentrations of both reactants at the catalyst surface are given is also studied. Simulations were performed using the finite difference technique. The influence of the size of the catalytic particle, surface diffusivity, adsorption rate constants, and particle jump rate constants via the catalyst-support interface on the catalytic reactivity of the supported catalyst is studied.

Keywords Heterogeneous reactions · Adsorption · Desorption · Surface diffusion · Spillover

1 Introduction

The surface of real catalysts consist of small metal catalyst particles placed on inactive supports. The metal particles are active in reaction whereas the reaction cannot occur on

V. Skakauskas (✉) · P. Katauskis
Faculty of Mathematics and Informatics, Vilnius University, Naugarduko 24,
03225 Vilnius, Lithuania
e-mail: vladas.skakauskas@maf.vu.lt

the support. One of kinetic effects associated with small catalyst particles on a support is the spillover phenomenon which plays a key role in catalytic reactions on supported catalysts [1,2]. It is caused by the fact that parts of the surface that are inactive in the surface reaction can be active for other processes that occur during the catalytic reaction, i.e. adsorption–desorption process and increase or decrease concentrations of either adsorbed reactant or product particles on active parts of the surface through the diffusion of the adsorbed reactant particles across the interface between the catalyst particles and the support [2,3].

The bibliography of the current state of the theoretical research of reactions with spillover effects include papers based on the Monte Carlo simulations technique, numerical solving of mean-field models, and analytical description of such effects. We mention papers devoted to study of the spillover effect in the unimolecular, $A \rightarrow P$, [3], monomer–monomer, $A + B \rightarrow AB$, [4,5], and monomer–dimer, $2A + B_2 \rightarrow 2AB$, [2,6–8] reactions. The latter models the CO oxidation reaction, $2CO + O_2 \rightarrow 2CO_2$, on the Pd/Al_2O_3 heterogeneous catalyst.

The dimer–dimer reactions, $2A_2 + B_2 \rightarrow 2A_2B$, proceeding on homogeneous surfaces have been studied by many groups (see [9–11] and references there). Reactions of this type are inspired by the catalytic oxydation of hydrogen on Pt catalysts. In papers [9–11] the diffusionless steady-state models are studied. In this paper, by employing a mean-field model and its numerical simulations we consider the time-dependent dimer–dimer reaction, $2A_2 + B_2 \rightarrow 2A_2B$, on supported (composite) catalysts. The model takes into account: the bulk diffusion of both reactants from a bounded vessel toward the adsorbent and the reaction product bulk one from the adsorbent into the same vessel, adsorption, desorption, and surface diffusion of adsorbed particles of each reactant. The model is based on the Langmuir–Hinshelwood surface reaction mechanism. The bulk diffusion of both reactants and product particles is described by the Fick law while the surface diffusion is based on the particle jumping mechanism [12]. Adsorption, desorption, surface diffusion and reaction are allowed to proceed at a constant temperature and the product desorption is assumed to be instantaneous. Lateral interactions between adsorbed particles or adsorbate-induced changes in the surface [13–15] have been neglected.

We consider two different arrangements of adsorption sites: (i) the same total amount of active and inactive in the surface reaction adsorption sites, (ii) the same concentrations of active and inactive adsorption sites. For each arrangement of adsorption sites we study two adsorption mechanisms of both reactants: (i) each reactant adsorbs on both active and inactive adsorption sites, (ii) both reactants adsorb only on the support. The goal of this paper is the numerical study of the surface diffusivity, adsorption rate constants, particle jump rate constants via catalyst-support interface, and catalytic particle size influence on the catalytic reactivity of supported catalysts.

The paper is organized as follows. In Sect. 2 we present the model. In Sect. 3 we discuss numerical results. A summary of main results in Sect. 4 concludes the paper.

2 The model

We study the dimer–dimer heterogeneous reaction, $2A_2 + B_2 \to 2A_2B$, proceeding on supported catalysts by using a mean-field approach. Assume that reactants A_2, B_2 and their reaction product $P = A_2B$ of concentrations $a(t,x)$, $b(t,x)$, and $p(t,x)$ occupy a bounded domain $\Omega = \{x = (x_1, x_2, x_3) : x_i \in [0, l],\ i = 1, 2, 3\}$ with boundary $\tilde{S} = S_1 \cup S_2$, where $S_2 = \{x = (x_1, x_2, x_3) : x_i \in [0, l],\ i = 1, 3, x_2 = 0\}$ and $S_1 = \tilde{S} \setminus S_2$. Here t is time, x is a position, S_2 is the surface of the adsorbent, and S_1 is a surface impermeable to the reactants and product. Obviously, $x_2 > 0$ for S_1.

Assume that $S_2 = S_{22} \cup S_{21}$ where $S_{22} = \{(x_1, x_2, x_3): x_1 \in [0, x_*),\ x_2 = 0,\ x_3 \in [0, l]\}$ and $S_{21} = \{(x_1, x_2, x_3): x_1 \in (x_*, l],\ x_2 = 0,\ x_3 \in [0, l]\}, x_* \in (0, l)$, are strips consisting of the active and inactive sites, respectively. Let $s_2(x)$, $x = (x_1, x_3) \in S_{22}$, and $s_1(x)$, $x = (x_1, x_3) \in S_{21}$, be the surface densities of the active and inactive sites in the surface reaction.

According [9,11] the surface reaction $2A_2 + B_2 \to 2A_2B$ occurs via steps

$$\begin{cases} A_2 + 2S \underset{k_{-1j}}{\overset{k_{1j}}{\rightleftarrows}} 2AS, \\ B_2 + 2S \underset{k_{-2j}}{\overset{k_{2j}}{\rightleftarrows}} 2BS, \\ AS + BS \xrightarrow{k_3} ABS + S, \\ AS + ABS \xrightarrow{k_4} P + 2S, \\ 2ABS \xrightarrow{k_5} P + BS + S. \end{cases} \tag{1}$$

Here A_2 and B_2 are reactants, $P = A_2B$ is their reaction product, S is the adjacent vacant adsorption site, k_{ji} and k_{-ji} are the adsorption and desorption rates constants ($i = 1$ for inactive site, $i = 2$ for active one), of reactants A ($j = 1$) and B ($j = 2$), k_3 is the reaction between adsorbates AS and BS rate constant in Langmuir–Hinshelwood step, k_4 is the reaction between adsorbate AS and intermediate ABS rate constant, and k_5 is the conversion rate constant of ABS into product P. This model is inspired by the catalytic oxidation of hydrogen on transition metal surfaces, i.e., $A_2 = H_2$, $B_2 = O_2$, $AB = OH$, $P = A_2B = H_2O$.

Let $u_{j2} = s_2\theta_{j2}$ and $u_{j1} = s_1\theta_{j1}$ ($\theta_{j1},\ \theta_{j2} \in (0, 1),\ j = 1, 2, 3$) be densities of the active and inactive in the surface reaction sites occupied by the adsorbed molecules of reactants A ($j = 1$) and B ($j = 2$), and particles of intermediate ABS ($j = 3$). Obviously, $s_i(1-\theta_{1i}-\theta_{2i}-\theta_{3i})$, $i = 1, 2$, are the densities of the free adsorption sites. It is evident that function u_{ji} present a density of particles of species AS, BS, and ABS bound to sites of type i ($i = 1$ for inactive and $i = 2$ for active site) that are located at point x.

Let κ_{ji} be the surface diffusivity for particles of adsorbates AS ($j = 1$), BS ($j = 2$) and intermediate ABS ($j = 3$) on the surface S_{2i}, $i = 1, 2$. To simplify the model we restrict ourselves to the case where densities s_1 and s_2 do not depend on variable x_3 and the initial values a^0 and b^0 of concentrations a and b are constants. In this case we can reduce the three-dimensional problem into two-dimensional one. Let $\lambda_{1,12}$, $\lambda_{1,22}$, and $\lambda_{1,32}$ be the constants of the jump rates via the catalyst-support interface x_* of

escaped particles of species *AS*, *BS*, and *ABS* from the active position $x_* - 0$ into the nearest-neighbour vacant inactive site $x_* + 0$. Similarly, $\lambda_{2,11}$, $\lambda_{2,21}$, and $\lambda_{2,31}$ are the constants of the jump rates via the catalyst-support of escaped particles of species AS, *BS*, and *ABS* from the inactive position $x_* + 0$ into the nearest-neighbour vacant active site $x_* - 0$. Assuming that product desorption is instantaneous and using mass action law and the surface diffusion mechanism based on the particle jumping into a nearest vacant adsorption site [12],

$$q_{ji} = -\kappa_{ji}\left\{(s_i - u_{1i} - u_{2i} - u_{3i})\nabla u_{ji} - u_{ji}\nabla(s_i - u_{1i} - u_{2i} - u_{3i})\right\},$$

we get the following system for densities u_{ji}:

$$\begin{cases} \partial_t u_{11} = 2\left(k_{11}a(s_1 - u_{11} - u_{21} - u_{31})^2 - k_{-11}u_{11}^2\right) \\ \quad + \kappa_{11}\left((s_1 - u_{21} - u_{31})\frac{\partial^2 u_{11}}{\partial x_1^2} - u_{11}\frac{\partial^2(s_1 - u_{21} - u_{31})}{\partial x_1^2}\right), \\ \partial_t u_{21} = 2\left(k_{21}b(s_1 - u_{11} - u_{21} - u_{31})^2 - k_{-21}u_{21}^2\right) \\ \quad + \kappa_{21}\left((s_1 - u_{11} - u_{31})\frac{\partial^2 u_{21}}{\partial x_1^2} - u_{21}\frac{\partial^2(s_1 - u_{11} - u_{31})}{\partial x_1^2}\right), \\ \partial_t u_{31} = \kappa_{31}\left((s_1 - u_{11} - u_{21})\frac{\partial^2 u_{31}}{\partial x_1^2} - u_{31}\frac{\partial^2(s_1 - u_{11} - u_{21})}{\partial x_1^2}\right) \end{cases} \tag{2}$$

with $x_1 \in (x_*, l)$,

$$\begin{cases} \partial_t u_{12} = 2\left(k_{12}a\left(s_2 - u_{12} - u_{22} - u_{32}\right)^2 - k_{-12}u_{12}^2\right) - k_3 u_{12}u_{22} \\ \quad - k_4 u_{12}u_{32} + \kappa_{12}\left(\left(s_2 - u_{22} - u_{32}\right)\frac{\partial^2 u_{12}}{\partial x_1^2} - u_{12}\frac{\partial^2\left(s_2 - u_{22} - u_{32}\right)}{\partial x_1^2}\right), \\ \partial_t u_{22} = 2\left(k_{22}b(s_2 - u_{12} - u_{22} - u_{32})^2 - k_{-22}u_{22}^2\right) - k_3 u_{12}u_{22} \\ \quad + k_5 u_{32}^2 + \kappa_{22}\left(\left(s_2 - u_{12} - u_{32}\right)\frac{\partial^2 u_{22}}{\partial x_1^2} - u_{22}\frac{\partial^2(s_2 - u_{12} - u_{32})}{\partial x_1^2}\right), \\ \partial_t u_{32} = k_3 u_{12}u_{22} - k_4 u_{12}u_{32} - 2k_5 u_{32}^2 \\ \quad + \kappa_{32}\left(\left(s_2 - u_{12} - u_{22}\right)\frac{\partial^2 u_{32}}{\partial x_1^2} - u_{32}\frac{\partial^2(s_2 - u_{12} - u_{22})}{\partial x_1^2}\right) \end{cases} \tag{3}$$

with $x_1 \in (0, x_*)$. Here ∂_t signifies the partial derivative with respect to time, ∇ is the gradient operator, q_{ji} is the surface diffusion flux of species AS ($j = 1$), BS ($j = 2$), ABS ($j = 3$) on the active ($i = 2$) and inactive ($i = 1$) interval, respectively. We add to this system the initial,

$$u_{ji}(0, x_1) = 0, \quad j = 1, 2, 3,\ i = 1, 2, \tag{4}$$

and boundary conditions at points $x_1 = 0,\ x_1 = l, x_1 = x_*$,

$$\begin{cases} \left.\dfrac{\partial u_{12}}{\partial x_1}\right|_{x_1=0} = \left.\dfrac{\partial u_{22}}{\partial x_1}\right|_{x_1=0} = \left.\dfrac{\partial u_{32}}{\partial x_1}\right|_{x_1=0} = 0, \\ \left.\dfrac{\partial u_{11}}{\partial x_1}\right|_{x_1=l} = \left.\dfrac{\partial u_{21}}{\partial x_1}\right|_{x_1=l} = \left.\dfrac{\partial u_{31}}{\partial x_1}\right|_{x_1=l} = 0, \end{cases} \tag{5}$$

$$\begin{cases} \kappa_{11}\left(\left(s_1-u_{21}-u_{31}\right)\frac{\partial u_{11}}{\partial x_1} - u_{11}\frac{\partial\left(s_1-u_{21}-u_{31}\right)}{\partial x_1}\right)\Big|_{x_*+0} \\ \quad = \kappa_{12}\left(\left(s_2-u_{22}-u_{32}\right)\frac{\partial u_{12}}{\partial x_1} - u_{12}\frac{\partial(s_2-u_{22}-u_{32})}{\partial x_1}\right)\Big|_{x_*-0} \\ \quad = \lambda_{2,11}\,u_{11}|_{x_*+0}\left(s_2-u_{12}-u_{22}-u_{32}\right)|_{x_*-0} \\ \qquad - \lambda_{1,12}\,u_{12}|_{x_*-0}\left(s_1-u_{11}-u_{21}-u_{31}\right)|_{x_*+0}, \\ \kappa_{21}\left(\left(s_1-u_{11}-u_{31}\right)\frac{\partial u_{21}}{\partial x_1} - u_{21}\frac{\partial\left(s_1-u_{11}-u_{31}\right)}{\partial x_1}\right)\Big|_{x_*+0} \\ \quad = \kappa_{22}\left(\left(s_2-u_{12}-u_{32}\right)\frac{\partial u_{22}}{\partial x_1} - u_{22}\frac{\partial\left(s_2-u_{12}-u_{32}\right)}{\partial x_1}\right)\Big|_{x_*-0} \\ \quad = \lambda_{2,21}\,u_{21}|_{x_*+0}\left(s_2-u_{12}-u_{22}-u_{32}\right)|_{x_*-0} \\ \qquad - \lambda_{1,22}\,u_{22}|_{x_*-0}\left(s_1-u_{11}-u_{21}-u_{31}\right)|_{x_*+0}, \\ \kappa_{31}\left(\left(s_1-u_{11}-u_{21}\right)\frac{\partial u_{31}}{\partial x_1} - u_{31}\frac{\partial\left(s_1-u_{11}-u_{21}\right)}{\partial x_1}\right)\Big|_{x_*+0} \\ \quad = \kappa_{32}\left(\left(s_2-u_{12}-u_{22}\right)\frac{\partial u_{32}}{\partial x_1} - u_{32}\frac{\partial\left(s_2-u_{12}-u_{22}\right)}{\partial x_1}\right)\Big|_{x_*-0} \\ \quad = \lambda_{2,31}\,u_{31}|_{x_*+0}\left(s_2-u_{12}-u_{22}-u_{32}\right)|_{x_*-0} \\ \qquad - \lambda_{1,32}\,u_{32}|_{x_*-0}\left(s_1-u_{11}-u_{21}-u_{31}\right)|_{x_*+0}. \end{cases} \tag{6}$$

The first terms (gain fluxes) on the right-hand side of Eq. (6) are conditioned by the jumps via the catalyst-support interface x_* of the escaped molecules of adsorbates *AS*, *BS*, and intermediate *ABS* from the inactive position, $x_* + 0$, of the support to the nearest-neighbour vacant active one, $x_* - 0$, of the catalyst. Similarly, the other terms (loss fluxes) on the right-hand side of Eq. (6) are conditioned by the jumps via the catalyst-support interface of the escaped molecules of the same species from the active position $x_* - 0$ of the catalyst to the nearest-neighbour vacant inactive one, $x_* + 0$, of the support.

Systems (2) and (3) involve the unknown values of concentrations a and b at the catalyst surface. To solve this problem we join equations for the bulk diffusion of both reactants,

$$\begin{cases} \partial_t a = \kappa_a\left(\dfrac{\partial^2 a}{\partial x_1^2} + \dfrac{\partial^2 a}{\partial x_2^2}\right), \quad (x_1, x_2) \in (0, l) \times (0, l), \\ \partial_n a|_{S_1} = 0, \\ \partial_n a = -\left(k_{11}a\left(s_1-u_{11}-u_{21}-u_{31}\right)^2 - k_{-11}u_{11}^2\right)/\kappa_a, \\ \quad x_1 \in (x_*, l),\ x_2 = 0, \\ \partial_n a = -\left(k_{12}a\left(s_2-u_{12}-u_{22}-u_{32}\right)^2 - k_{-12}u_{12}^2\right)/\kappa_a, \\ \quad x_1 \in (0, x_*),\ x_2 = 0, \\ a(0, x) = a_0(x), \quad (x_1, x_2) \in (0, l) \times (0, l), \end{cases} \tag{7}$$

$$\begin{cases} \partial_t b = \kappa_b \left(\frac{\partial^2 b}{\partial x_1^2} + \frac{\partial^2 b}{\partial x_2^2} \right), \quad (x_1, x_2) \in (0, l) \times (0, l), \\ \partial_n b|_{S_1} = 0, \\ \partial_n b = -\left(k_{21} b (s_1 - u_{11} - u_{21} - u_{31})^2 - k_{-21} u_{21}^2 \right) / \kappa_b, \\ \quad x_1 \in (x_*, l), \ x_2 = 0, \\ \partial_n b = -\left(k_{22} b (s_2 - u_{12} - u_{22} - u_{32})^2 - k_{-22} u_{22}^2 \right) / \kappa_b, \\ \quad x_1 \in (0, x_*), \ x_2 = 0. \\ b(0, x) = b_0(x), \quad (x_1, x_2) \in (0, l) \times (0, l). \end{cases} \tag{8}$$

Here $\partial_n a$ and $\partial_n b$ are the outward normal derivatives. We describe the bulk diffusion of product P by the equations

$$\begin{cases} \partial_t p = \kappa_p \left(\frac{\partial^2 p}{\partial x_1^2} + \frac{\partial^2 p}{\partial x_2^2} \right), \quad (x_1, x_2) \in (0, l) \times (0, l), \\ \partial_n p|_{S_1} = 0, \\ \partial_n p = (k_5 u_{32}^2 + k_4 u_{12} u_{32}) / \kappa_p, \quad x_1 \in (0, x_*), \ x_2 = 0, \\ \partial_n p = 0, \quad x_1 \in (x_*, l), \ x_2 = 0, \\ p(0, x) = 0, \quad (x_1, x_2) \in (0, l) \times (0, l). \end{cases} \tag{9}$$

System (2)–(9) possesses two conservation laws

$$\int_\Omega (2a + 2p)\, \mathrm{d}x + \int_0^{x_*} (u_{12} + u_{32})\, \mathrm{d}x_1 + \int_{x_*}^{l} (u_{11} + u_{31})\, \mathrm{d}x_1 = \int_\Omega 2a_0\, \mathrm{d}x, \tag{10}$$

$$\int_\Omega (2b + p)\, \mathrm{d}x + \int_0^{x_*} (u_{22} + u_{32})\, \mathrm{d}x_1 + \int_{x_*}^{l} (u_{21} + u_{31})\, \mathrm{d}x_1 = \int_\Omega 2b_0\, \mathrm{d}x. \tag{11}$$

Coupled system (2)–(9) determines densities u_{ji} (or surface coverages θ_{ji}) for all $x \in S_2$ and concentrations a, b, and p of reactants A, B and product P for all $x \in \Omega$ and $t > 0$.

We also study system (2)–(6) with given concentrations a and b at the surface S_2.

The main characteristic that we study is the surface S_{22} specific conversion rate of the reactants molecules into the product ones (turn-over rate or turn-over frequency) determined by the formula

$$z = \int_0^{x_*} \left(k_5 u_{32}^2 + k_4 u_{12} u_{32} \right) \mathrm{d}x_1 \Big/ \int_0^{x_*} s_2\, \mathrm{d}x_1. \tag{12}$$

Using the dimensionless variables $\bar{t} = t/T$, $\bar{x}_i = x_i/l$, $\bar{a} = a/a_*$, $\bar{b} = b/a_*$, $\bar{p} = p/a_*$, $\bar{s}_i = s_i/s_*$, $s_* = l a_*$, $\bar{k}_{in} = k_{in} T l a_*^2$, $\bar{k}_{-in} = k_{-in} T l a_*$, $\bar{k}_3 = k_3 T l a_*$, $\bar{k}_4 = k_4 T l a_*$, $\bar{k}_5 = k_5 T l a_*$, $\bar{\kappa}_{ji} = \kappa_{ji} a_* T / l$, $\bar{\kappa}_a = \kappa_a T / l^2$, $\bar{\kappa}_b = \kappa_b T / l^2$, $\bar{\kappa}_p =$

$\kappa_p T/l^2$, $\bar{\lambda}_{n,ji} = a_* T\,\lambda_{n,ji}$, $\bar{u}_{ji} = \bar{s}_i\theta_{ji}$ where $i = 1, 2$, $j = 1, 2, 3$, $n = 1, 2$, and T, l, a_* are the characteristic dimensional units, we rewrite Eqs. (2)–(12) in the same form, but in dimensionless variables where dimensionless $l = 1$. We omit the overbar on the quantities and treat Eqs. (2)–(12) as dimensionless for simplicity.

3 Numerical results

System (2)–(6) with given values of a and b at the surface S_2 was solved numerically using an implicit difference scheme. To solve system (2)–(9) numerically we used an implicit difference scheme based on the alternating direction method [16]. For all calculations we used the following model dimensional data:

$$\begin{aligned}
&T = 1\ \mathrm{s}, \quad l = 10^{-1}\ \mathrm{cm}, \quad a_* = 10^{-11}\ \mathrm{mol\,cm^{-3}},\\
&s_* = 10^{-12}\ \mathrm{mol\,cm^{-2}}, \quad k_{in} = \bar{k}_{in}\cdot 10^{23}\ \mathrm{cm^5\,mol^{-2}\,s^{-1}},\\
&k_{-in} = \bar{k}_{-in}\cdot 10^{12}\ \mathrm{cm^2\,mol^{-1}\,s^{-1}},\\
&\quad(\kappa_a, \kappa_b, \kappa_p) = (\bar{\kappa}_a, \bar{\kappa}_b, \bar{\kappa}_p)\cdot 10^{-2}\ \mathrm{cm^2\,s^{-1}},\\
&\kappa_{ji} = \bar{\kappa}_{ji}\cdot 10^{10}\ \mathrm{mol^{-1}\,cm^4\,s^{-1}},\\
&\lambda_{n,ji} = \bar{\lambda}_{n,ji}\cdot 10^{11}\ \mathrm{mol^{-1}cm^3s^{-1}},\\
&\quad(k_3, k_4, k_5) = (\bar{k}_3, \bar{k}_4, \bar{k}_5)\cdot 10^{12}\ \mathrm{mol^{-1}cm^2s^{-1}}
\end{aligned} \tag{13}$$

The following values of dimensionless parameters (overbar on the quantities is omitted) excluding those given in captions were used in calculations:

$$\begin{aligned}
&k_{ji} = 1.5\cdot 10^{-2}, \quad k_{-ji} = 1.5\cdot 10^{-3},\\
&\kappa_{ji} = 0.5, \quad \lambda_{n,ji} = 0.1, \quad j = 1, 2, 3,\ i = 1, 2,\ n = 1, 2,\\
&k_3 = k_4 = k_5 = 0.1,\\
&\kappa_a = \kappa_b = \kappa_p = 0.1,\\
&x_* = 0.5.
\end{aligned} \tag{14}$$

In the case where values of k_{ji}, κ_{ji}, and $\lambda_{n,ji}$ do not depend on the specific values of indices we use k, κ, and λ for short. Of course, the case where k_{ji}, κ_{ji}, and $\lambda_{n,ji}$ do not depend on values of indices is not realistic. However, it is useful for study of many different physico-chemical processes. As we indicated in Sect. 2, the main purpose of our study was to estimate the turn-over rate $z(t)$. Numerical results are illustrated in Figs. 1, 2, 3, 4, 5, and 6. Figs. 1, 2 and 3 correspond to Eqs. (2)–(6) with given values of concentrations a and b at the catalyst surface S_2, while the other three figures illustrate dynamics of $z(t)$ determined by Eqs. (2)–(8). In calculations we used two types of adsorption sites arrangement: (i) the same total amount of active and inactive adsorption sites, i.e. (i) $s_2 x_* = s_1(1 - x_*)$, (ii) $s_1 = s_2$.

Figure 1 illustrates the dependence of the turn-over rate $z(t)$ on the variation of size x_* of the catalyst particle for both arrangements of adsorption sites (solid lines correspond to the same total amount of active and inactive adsorption sites while the

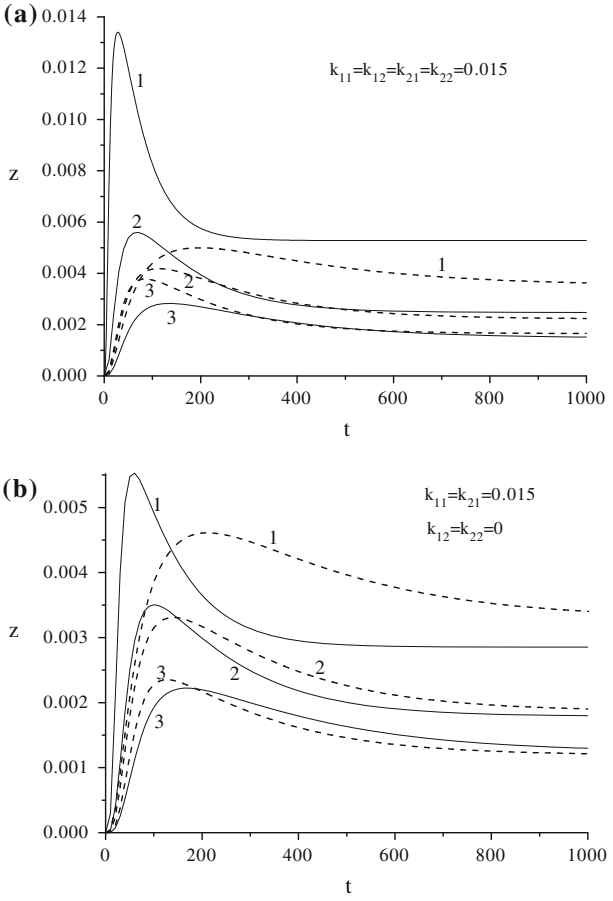

Fig. 1 Influence of the active interval length x_* on the turnover rate $z(t)$ determined by Eqs. (2)–(6) with $a = b = 1$ at the surface S_2 for densities $s_2 = s_1(1/x_* - 1)$, $s_1 = 1$ (*solid line*) and $s_1 = s_2 = 1$ (*dashed line*) in the case $\kappa = 0.5$, $\lambda = 0.1$. Values of x_*: 0.2 (*1*), 0.4 (*2*), 0.6 (*3*)

dashed lines illustrate the behaviour of $z(t)$ determined for the same concentrations of active and inactive sites) in the case where reaction rate constants $k_3 = k_4 = k_5 = 0.1$, bulk diffusivity $\kappa = 0.5$, particle jump rate constant via the interface of the catalyst-support $\lambda = 0.1$, adsorption rate constant $k = 1.5 \cdot 10^{-2}$ (Fig. 1a) and $k_{12} = k_{22} = 0$, $k_{11} = k_{21} = 1.5 \cdot 10^{-2}$ (Fig. 1b). Values of adsorption rate constants show that Fig. 1b correspond to the case where active in the surface reaction sites are adsorption-inactive. In this case the surface reactions proceeds only due to spillover phenomenon. The qualitative behaviour of $z(t)$ (see Fig. 1a, b) is similar in both cases of the adsorption rate constants (solid lines) or both types of adsorption sites arrangements (dashed lines). For all t, $z(t)$ grows as size x_* decreases. For fixed values of parameters, $z(t)$ also grows as time increases, reaches a maximum value and then decreases to a positive stationary value. In the case of small x_* and $s_1 = s_2$ the peak of $z(t)$ is not so sharp as that corresponding to $s_2 = s_1(1/x_* - 1)$. Moreover, for small time in the case of

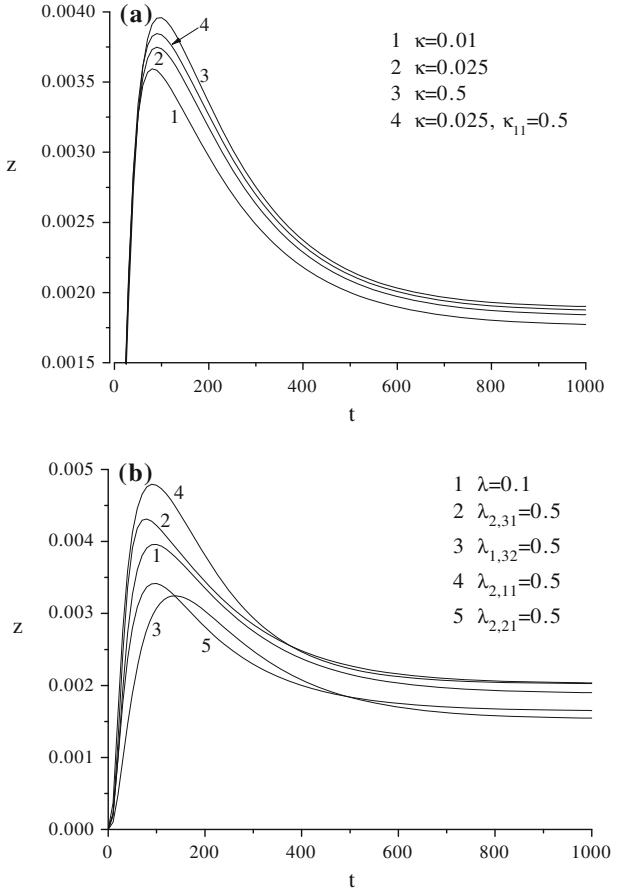

Fig. 2 Effect of surface diffusivity κ (**a**) and jump rate constants $\lambda_{i,jn}$ (**b**) on function $z(t)$ determined by (2)–(6) with $a = b = 1$ at the surface S_2 in case $s_2 = s_1(1/x_* - 1)$, $s_1 = 1$. $\lambda_{i,jn} = 0.1$ for all values of indices excluding those given in the figure

small adsorption rate constants k_{12}, k_{22} and $x_* < 0.5$, values of $z(t)$ corresponding to $s_2 = s_1(1/x_* - 1)$ are larger than those corresponding to $s_2 = s_1$, while for large time or $x_* > 0.5$ the behaviour of $z(t)$ is opposite. In case of large k_{12}, k_{22} and small x_*, $z(t)$ corresponding to $s_2 = s_1(1/x_* - 1)$ is larger than that determined by $s_2 = s_1$ for all t.

Figure 2 depicts the influence of the variation of the surface diffusivity κ (Fig. 2a) and particle jump rate constant $\lambda_{n,ji}$ (Fig. 2b) for $x_* = 0.5$, $k_3 = k_4 = k_5 = 0.1$, $k = 1.5 \cdot 10^{-2}$, and $k_{-ji} = 1.5 \cdot 10^{-3}$ with all values of indices. Figure 2a shows the increase of $z(t)$ as κ grows and also demonstrates the nonmonotonic behaviour of $z(t)$ in time. As in Fig. 1 for fixed values of parameters, $z(t)$ increases as time grows, reaches a maximum value, and then decreases to a positive stationary value. Calculations show an insignificant influence of the variation of κ_{2i} or κ_{3i}, $i = 1, 2$, and κ_{12} on the behaviour of $z(t)$. The dependence of $z(t)$ on κ_{11} is more appreciable. Plots

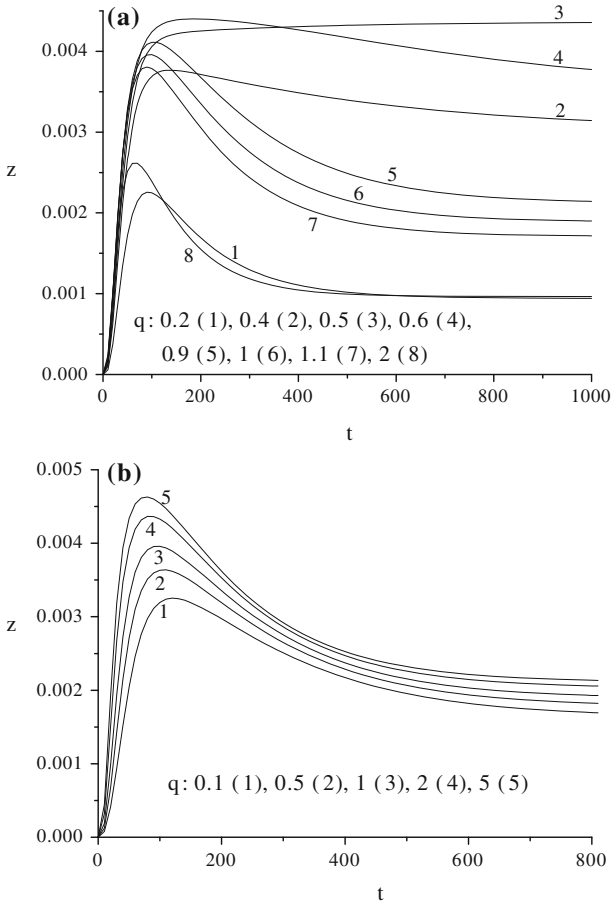

Fig. 3 Dependence of turnover rate $z(t)$ determined by (2)–(6) with $a = b = 1$ at the surface S_2 for densities $s_2 = s_1(1/x_* - 1)$, $s_1 = 1$ on the adsorption rate constants k_{ij}. **a** $k_{11} = k_{12} = 1.5 \cdot 10^{-2}$, $k_{21} = k_{22} = qk_{11}$. **b** $k_{12} = k_{22} = 1.5 \cdot 10^{-2}$, $k_{11} = k_{21} = qk_{12}$

in Fig. 2b demonstrate the increase of $z(t)$ as $\lambda_{2,31}$ or $\lambda_{2,11}$ grows and its decrease as $\lambda_{1,32}$ or $\lambda_{2,21}$ increases. The most essential is parameter $\lambda_{2,11}$.

The influence of adsorption rate constant k_{ji} on the behaviour of $z(t)$ is depicted in Fig. 3a, b for $x_* = 0.5$, $\kappa = 0.1$, $k_3 = k_4 = k_5 = 0.1$, and $k_{-ji} = 1.5 \cdot 10^{-3}$ with all values of indices. Plots in Fig. 3a correspond to the same value of the adsorption rate constant of reactant A on both active and inactive intervals, $k_{11} = k_{12} = 1.5 \cdot 10^{-2}$, and different values of common for both intervals adsorption rate constant of reactant B, $k_{21} = k_{22} = qk_{11}$, $q = 0.2, 0.4, 0.5, 0.6, 0.9, 1, 1.1, 2$. This figure shows the nonmonotonic behaviour of z in time for all values of q excluding value $q \neq 0.5$ for which $z(t)$ monotonically tends to an asymptotic value. For fixed q ($q \neq 0.5$) function $z(t)$ grows, reaches a maximum value, and then tends to a positive asymptotic value as time increases. Plots in this figure depict the increase of the asymptotic value of

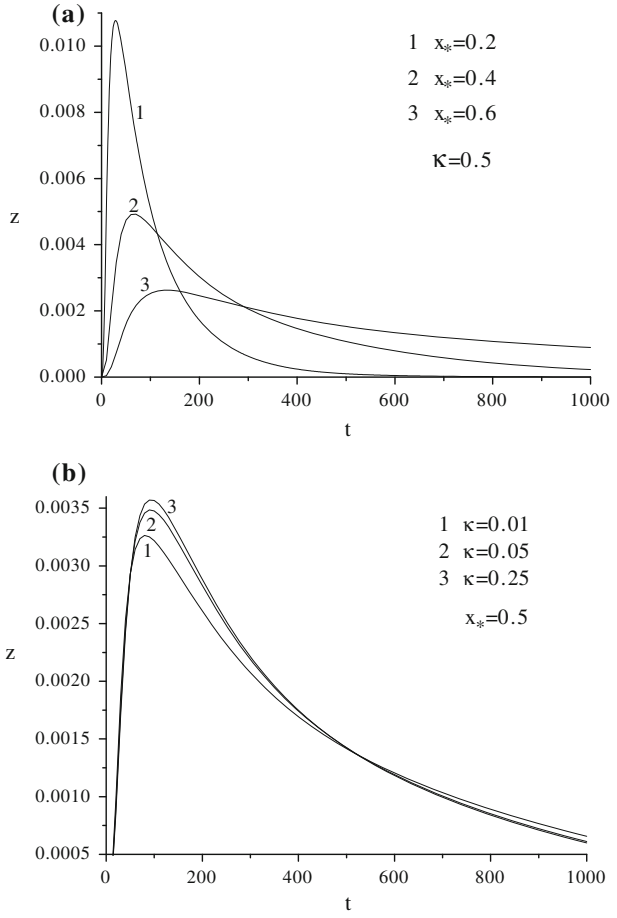

Fig. 4 Influence of the active interval length x_* (**a**) and surface diffusivity κ (**b**) on the turnover rate $z(t)$ determined by Eqs. (2)–(9) with densities $a_0(x_1, x_2) = b_0(x_1, x_2) = 1$ and $s_2 = s_1(1/x_* - 1)$, $s_1 = 1$

$z(t)$ as q grows till 0.5 where it reaches a maximum value. Then the asymptotic value $z(t)$ decreases as q grows. Calculations show that for large time and $q < 0.5$ or $q > 0.5$ the both active and inactive intervals are predominantly covered by particles of reactant A or B, respectively. The same results have been given in [9] for the case of homogeneous catalysts.

We also studied three additional cases: (i) $k_{11} = k_{12} = k_{22} = 1.5{\cdot}10^{-2}, k_{21} = qk_{11}$, (ii) $k_{11} = k_{12} = k_{21} = 1.5 \cdot 10^{-2}$, $k_{22} = qk_{11}$, (iii) $k_{12} = k_{21} = k_{22}$, $k_{11} = qk_{12}$. In the first case the maximal asymptotic value of z occurs at $q = 0$, but this value is smaller than the local maximum value of $z(t)$ reached at small time. In the second case, z monotonically increases to an asymptotic value only for $q \approx 0.1$. The difference between this value of z and that corresponding to $k_{11} = k_{12} = 1.5 \cdot 10^{-2}$, $k_{21} = k_{22} = 0.5k_{11}$ is smaller than 1% of the latter one. For $q \neq 0.1$, $z(t)$ behaves non-monotonically, i.e., reaches maximal value and then decreases to an asymptotic value.

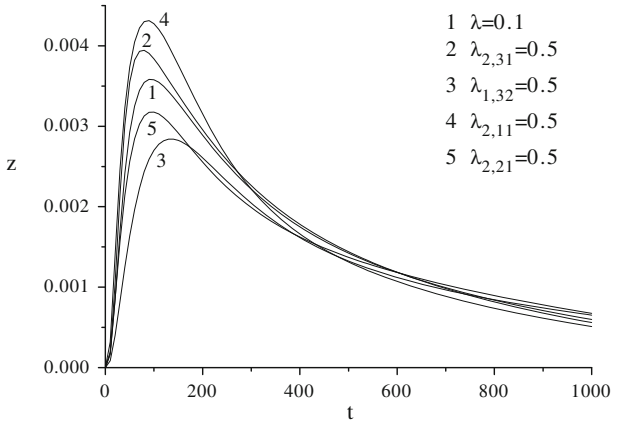

Fig. 5 Dependence of the turnover rate $z(t)$ determined by Eqs. (2)–(9) with densities $a_0(x_1, x_2) = b_0(x_1, x_2) = 1$ and $s_2 = s_1(1/x_* - 1)$, $s_1 = 1$ on the parameters $\lambda_{i,jn}$. $\lambda_{i,jn} = 0.1$ for all values of indices excluding those given in the figure

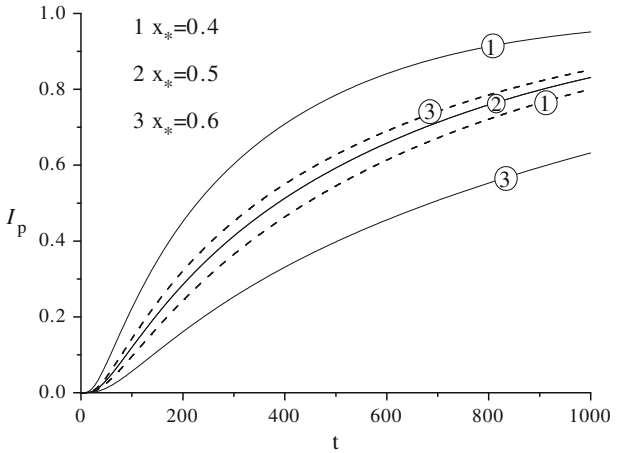

Fig. 6 Dependence of the total amount of the product I_p on the active interval length x_*. Densities $a_0(x_1, x_2) = b_0(x_1, x_2) = 1$ and $s_2 = s_1(1/x_* - 1)$, $s_1 = 1$—*solid line*, $s_1 = s_2 = 1$—*dashed line*

In the third case, $z(t)$ grows as q increases, but preserves nonmonotonic behaviour in time. This increase can be explained only by the spillover effect.

Plots in Fig. 3b illustrate the influence of the same adsorption rate constant of both reactants for the inactive interval, $k_{11} = k_{21} = qk_{12}$, $q = 0.1, 0.5, 1, 2, 5$, on the behaviour of $z(t)$ provided that the common adsorption rate constant of both reactants on the active interval $k_{12} = k_{22} = 1.5 \cdot 10^{-2}$. This figure demonstrates the substantial influence of the spillover effect on the monotonic growth of $z(t)$ as q increases and the nonmonotonic behaviour of $z(t)$ in time for all considered values of q.

We also compared the influence of reaction rate constants k_4 and k_5 on the behaviour of $z(t)$ determined by system (2)–(6) with given values of a and b at the surface S_2

in cases where (i) $k_4 = k_5 = 0.1$; (ii) $k_4 = 0$, $k_5 = 0.1$; and (iii) $k_4 = 0.1$, $k_5 = 0$. Calculations show that $z(t)$ determined for the third collection is between those corresponding to the first and second ones only for small time, while for large time $z(t)$ determined by the second collection is between those determined for the third and first ones. Moreover, the asymptotic values of z corresponding to the first and second collection of parameters are about 2.04 and 1.9, respectively, times larger than that corresponding to the third one, while the difference of the asymptotic values of z corresponding to the first and second collections of parameters is about 6.9 % of the first one.

Plots in Figs. 4 and 5 correspond to system (2)–(8) and are depicted for initial values $a_0 = b_0 = 1$ and the same total active and inactive in reaction adsorption sites. Figure 4 illustrates the dependence of $z(t)$ on the size x_* of catalytic particle (Fig. 4a) and surface diffusivity κ (Fig. 4b) for the same values of parameters as in Figs. 1a and 2a, respectively. Contrary to Fig. 1a, Fig. 4a demonstrates the increase of $z(t)$ as x_* grows only for small time. For large time, $z(t)$ behaves vice-versa and tends to zero as time grows. This effect can be explained by the depletion of mass of both reactants from domain Ω during reactions.

Plots in Fig. 5 illustrate the effect of particle jump rate constant $\lambda_{n,ji}$ on the behaviour of $z(t)$. We observe a similar nonmonotonic behaviour of plots in Figs. 2b and 5, but the later ones tend to zero as time grows, while all plots in Fig. 3 remain positive.

Figure 6 illustrates the influence of catalytic particle size x_* on the behaviour on the total product amount $I_p = \int_0^{x_*} \int_0^{x_*} p(t, x_1, x_2)\, \mathrm{d}x_1\, \mathrm{d}x_2$ for two types of the active sites arrangement. In the case of equal total amount of active and inactive adsorption sites, I_p grows as x_* decreases and behaves vice-versa in the case of equal concentrations of active and inactive adsorption sites.

4 Conclusions

To conclude the paper we summarise the main results. Using the phenomenological (mean-field) model in two-dimensional space we studied numerically dimer–dimer surface reactions of type $2A_2 + B_2 \rightarrow 2A_2B$ proceeding on supported catalysts taking into account the bulk diffusion of both reactants and product in a bounded vessel. The model includes the adsorption, desorption, surface diffusion of adsorbed particles of each reactant, and rapid product desorption from the surface. The model where concentrations of both reactants at the catalyst surface are given is also studied. To describe the surface diffusion the particle jumping mechanism [12] was applied. Two different arrangements of adsorption sites were used: (i) the same total amount of active and inactive in reaction adsorption sites, (ii) the same concentrations of active and inactive in reaction adsorption sites. Two adsorption mechanisms of both reactants for each arrangement of adsorption sites are considered: (i) each reactant adsorbs on both active and inactive in reaction adsorption sites, (ii) both reactants adsorb only on the support.

Inactive in reaction adsorption sites due to possibility to adsorb of particles of both reactants constitute the additional (to the adsorption) spillover channel transporting particles onto active ones.

The main characteristic we studied was the turn-over rate (specific conversion rate of molecules of both reactants into the product particles). We analysed the spillover effect on the turn-over rate and demonstrated that:

1. The size of active interval x_* strongly influences the turn-over rate. In both cases of adsorption sites arrangement, $z(t)$ determined by Eqs. (2)–(6) with given values of concentrations of both reactants at the catalyst surface or (2)–(8) grows as size x_* decreases. Moreover, for small time, in the case of small adsorption rate constants k_{12}, k_{22} and $x_* < 0.5$, values of $z(t)$ corresponding to $s_2 = s_1(1/x_* - 1)$ are larger than those corresponding to $s_2 = s_1$, while for large time or $x_* > 0.5$ the behaviour of $z(t)$ is opposite.
2. The increase of diffusivity κ increases $z(t)$ corresponding to system (2)–(6) with given a and b at the catalyst surface for all time, while $z(t)$ determined by Eqs. (2)–(8) grows as κ only for small time. For large time it behaves vice-versa.
3. $z(t)$ increases as $\lambda_{2,31}$ or $\lambda_{2,11}$ grows and decreases as $\lambda_{1,32}$ or $\lambda_{2,21}$ increases. The most essential is parameter $\lambda_{2,11}$.
4. The asymptotic value of $z(t)$ as a function of $k_{21} = k_{22}$ has maximum at the point $k_{21} = k_{22} = 0.5k_{11}$, $k_{11} = k_{12} = 1.5 \cdot 10^{-2}$ which is larger than $z(t)$ for any t. Function $z(t)$ also preserves the similar behaviour in the case where $k_{11} = k_{12} = k_{21} = 1.5 \cdot 10^{-2}$, $k_{22} = 0.1k_{11}$.
5. Asymptotic values of z determined by system (2)–(6) with the surface reaction step with $k_4 = 0$ and positive k_5 are much more larger than those corresponding to the step where $k_5 = 0$ and $k_4 > 0$.

Results of simulations let us to think that the mean-field model presented here is able to describe qualitatively processes proceeding at the constant temperature during dimer–dimer reactions on supported catalysts.

Acknowledgments This work was supported by the Research Council of Lithuania (Project No. MIP-052/2012).

References

1. V.P. Zhdanov, B. Kasemo, Surf. Sci. Rep. **39**, 25 (2000)
2. L. Cwiklik, B. Jagoda-Cwiklik, M. Frankowitz, Appl. Surf. Sci. **252**, 778 (2005)
3. T.G. Mattos, F.D.A. Aarão Reis, J. Catal. **263**, 67 (2009)
4. V. Skakauskas, P. Katauskis, J. Math. Chem. **51**, 1654 (2013)
5. V. Skakauskas, P. Katauskis, J. Math. Chem. **52**, 1350 (2014)
6. V.P. Zhdanov, B. Kasemo, J. Catal. **170**, 377 (1997)
7. E.V. Kovaliov, E.D. Resnyanskii, V.I. Elokhin, B.S. Bal'zhinimaev, A.V. Myshlyatsev, Phys. Chem. Chem. Phys. **5**, 784 (2003)
8. V.P. Zhdanov, B. Kasemo, Surf. Sci. **405**, 27 (1998)
9. B. Hellsing, B. Kasemo, V.P. Zhdanov, J. Catal. **132**, 210 (1991)
10. E.V. Albano, J. Phys. A Math. Gen. **25**, 2557 (1992)
11. A. Maltz, E.V. Albano, Surf. Sci. **277**, 414 (1992)
12. A.N. Gorban, H.P. Sargsyan, H.A. Wahab, Math. Model. Nat. Phenom. **6**, 184 (2011)
13. V.P. Zhdanov, Surf. Sci. **209**, 523 (1989)
14. V.P. Zhdanov, Surf. Sci. **219**, L571 (1989)
15. V.P. Zhdanov, J. Phys. Chem. **93**, 5582 (1989)
16. A.A. Samarskii, *The Theory of Difference Schemes* (Marcel Dekker, New York, 2001)